Green Synthesis of Copper Manganese Oxide Nanoparticles from Ginkgo Biloba Extract and Study of their Activity on PC3 Cancer Cell Line

Heba Jassim Younis[1], Mustafa Hammadi[1] and Rulla Sabah[2]
[1]*Department of Chemistry, College of Education for Pure Science, University of Diyala, 32001 Diyala, Iraq*
[2]*Department of Chemistry, Faculty of Science, Mustansiriyah University, 10064 Baghdad, Iraq*
{hiba.y.jasim.msc23, mustafa.hameed}@uodiyala.edu.iq, rulla_sabah77@uomustansiriyah.edu.iq

Keywords: Green Synthesis, Copper Manganese Oxide with Composition, Nanoparticles, Ginkgo Biloba, Flutamide PC3 Cell.

Abstract: This study presents a novel, cost-effective method for synthesizing $Cu_{1.4}Mn_{1.6}O_4$ nanoparticles utilizing Ginkgo Biloba leaf extract. The approach integrates green chemistry, co-precipitation, and ultrasound techniques into a single methodology for nanoparticle preparation. The prepared nanoparticles underwent characterization through various techniques, including XRD, FT-IR, EDX, SEM, and DLS. While the average size noted in the XRD was 38.12 nm, the average particle size observed in the SEM was 103.60 nm. The average particle size measured by DLS was 196.3 nm. The efficacy of the synthesized $Cu_{1.4}Mn_{1.6}O_4$ nanoparticles was evaluated against the pharmaceutical Flutamide, utilized in Iraq for the treatment of prostate cancer, on the PC3 cell line. The results demonstrated the exceptional efficacy and superiority of the produced nanoparticles compared to the administered medication. Their characterization included reduced cytotoxicity relative to the drug's toxicity on red blood cells during the toxicity screening test, where $Cu_{1.4}Mn_{1.6}O_4$ exhibited cell killing rates of 37.68%, 47.75%, 63.38%, 87.07%, and 98.00%. results in 24 hours showed an IC50 value = 38.46; In contrast, Flutamide demonstrated cell-killing rates of 6.51%, 10.45%, 27.69%, 32.48%, and 52.53%and results showed an IC50 value of 296.8 at 24 hours too.

1 INTRODUCTION

Prostate cancer is a prevalent malignant neoplasm in males, primarily impacting prostate tissue. Crucially important for the male reproductive system, the prostate gland generates semen. Prostate cancer generally exhibits gradual growth, and its initial symptoms are ambiguous. It may induce symptoms including frequent urination, an urgent compulsion to urinate, and discomfort. As the illness advances, symptoms, including ostealgia, lethargy, and weight reduction, may manifest. Preventive strategies for prostate cancer encompass sustaining a healthy lifestyle, undergoing frequent examinations, and avoiding exposure to detrimental substances [1]. Numerous studies have shown that the development of prostate cancer is mostly dependent on growth factors, which either directly raise steroid hormone levels or, using an active feedback process, increase enzyme activity. Radiation therapy, surgery, and chemotherapy are the present choices for prostate cancer treatment. Treatment with conventional chemotherapy, which is often used to treat androgen-independent prostate cancer, can lead to resistance and progression, further complicating the situation given the lack of available treatment options [2]. Although it is the most successful cancer treatment, these chemotherapy drugs have numerous side effects due to their cytotoxic properties [3]. Furthermore, reducing the chance of cancer death and recurrence is the goal of radiation treatment. Usually, it entails radiation exposure to surrounding organs, which raises the risk of heart and lung illness. Particularly when used with some kinds of adjuvant chemotherapy [4], these therapies could raise leukemia risk. Wild plants and animals have long been the main source of natural remedies that have significantly improved human health. However, creating medications from these materials has grown more difficult due to continuous changes and human exploitation of wild ecosystems. Consequently, scientists are currently investigating the large ocean of alternative medicine sources [5].

For thousands of years, ginkgo biloba (Ginkgo Biloba L.) has been used as a Chinese herb to cure bronchitis and asthma [6]. In recent pharmacological studies, Ginkgo Biloba leaf extract (EGB) has shown anti-inflammatory, antioxidant, neuroprotective, anti-cardiovascular, and peripheral vascular properties in addition to its anti-platelet aggregation activities [9]. Terpene ticlatones and flavanol glycosides are their primary bioactive constituents [10]. Oncology nanotechnology can aid in updating cancer detection and treatment. Patients with breast cancer now have new hope thanks to the development of novel targeted technologies at the nanoscale made possible by advances in materials science and protein engineering [11]-[13]. Nanoparticles (NPs), sometimes called drug carriers, offer a novel way to deliver medications to cancer cells with great specificity for the targeted cancer cells by precisely penetrating tumours [14]. A novel class of nanomaterials called bimetallic nanoparticles (BNPs) comprises two distinct metallic components [15]. Their structure resembles that of monometallic counterparts in certain aspects; however, the synergistic interaction between the two components enables the manifestation of diverse novel properties and applications. BNPs have garnered considerable attention from researchers owing to their distinctive catalytic, electronic, optical, and magnetic properties [16]. Materials made of two metals that have unique properties because of their synergistic effects are called bimetallic nanoparticles. Compared to monometallic nanoparticles, bimetallic nanoparticles (nanoalloys) offer a greater potential for use [17]. Unlike chemical and physical methods, biosynthesis of bimetallic nanoparticles is a safe, reasonably priced, clean, ecologically benign technique [18]. Investigated and proven to be more effective than their monometallic counterparts are the anticancer capabilities of some bimetallic nanoparticles, including silver and gold, silver and copper, and zinc and silver [19]. A colon adenocarcinoma cell line (HT-29) was used in prior work to assess the anticancer effects of copper-manganese bimetallic nanoparticles (CMBNPs), which were produced from pumpkin seed extract [20]. Numerous studies have shown impressive anticancer efficacy against various cancer cell types using copper and manganese bimetallic nanoparticles. For instance, it has been documented that copper nanoparticles use oxidative stress and DNA damage to cause apoptosis and cell death and prevent the growth of cancer cells. Manganese nanoparticles have also shown promise in cancer treatment. They boost the formation of reactive oxygen species (ROS) in cancer cells, inducing death and cell cycle arrest [21]. Moreover, these nanoparticles' distinct physicochemical characteristics, including their size, shape, and surface modifications, can be altered to maximize their effectiveness against cancer cells and reduce their negative effects on healthy tissue [22]. These results highlight the potential of manganese and copper bimetallic nanoparticles as effective targets for anticancer treatment. Bimetallic copper and manganese nanoparticles have shown exceptional antibacterial efficacy against various pathogenic microbes in addition to their anticancer qualities. For instance, copper nanoparticles demonstrated strong antibacterial action by rupturing bacterial cell membranes and interfering with essential biological functions [23]. Manganese nanoparticles demonstrate significant efficacy as antimicrobial agents, especially against drug-resistant bacterial strains [24].

2 MATERIALS, TECHNIQUES AND METHODS

2.1 Items of Research

Cu (NO3)2, Molecular Weight=187.57 from Sigma-Aldrich Purity=98%, Mn(NO3)2, Molecular Weight=178.95 from Sigma-Aldrich Purity=99%, Deionized water from Iraq Babylon Purity=99%, Na2CO3, Molecular Weight=106.00 from Sigma Purity=98%, NaBH4 Molecular Weight=37.83 from Sigma-Aldrich Purity=99%, CH3CH2OH Molecular Weight=46. 07 from England (BDH), Purity=99%, Ginkgo biloba from Iraq Market, Flutamide tablets 20mg from ALIUD PHARMA(Germany).

2.2 Extraction of Ginkgo Biloba Leaf Extract

Combine 50g of Ginkgo biloba leaves with 500 ml of deionized water in a 10:1 ratio, stirring the mixture magnetically for one hour at 50°C. Subsequently, filter the mixture and store the filtrate in a cool location [25].

2.3 Synthesis of $Cu_{1.4}Mn_{1.6}O_4$ Nanoparticles by Green Chemical Methods

To create one molar, 3.75 grams of Cu (NO3)2 salts should be dissolved in 50 millilitres of ginkgo biloba

leaf extract. 3.57 grams should be dissolved in 50 millilitres of the extract to create one molar of Mn(NO3)2. Following a half-hour of mixing and 350 cycles at 40°C, the two solutions were put on the magnetic stirrer. Following ten minutes in an ultrasonic device, the mixture was placed on a magnetic stirrer, the pH was adjusted to 7, and the Na2CO3 solution was gradually added at a concentration of two molar. After that, NaBH4 was gradually added to it at a one-molar concentration. The precipitate was filtered and cleaned twice with ethanol and three times with deionized water. At 180°C, the residue was dried. The residue was then burnt for four hours at 650°C.

2.4 Approaches for Characterization

The $Cu_{1.4}Mn_{1.6}O_4$ Nanoparticles were analyzed using various methods. The nanoparticles' crystallite size was ascertained by XRD (Shimadzu, Kyoto, Japan). Shimadzu (Tokyo, Japan) was used to obtain the FTIR spectra of the materials. A 200 kV Zeiss SEM (Germany) was used for the SEM analysis. Anton Paar Litesizer DLS 100.

2.5 MTT Test for $Cu_{1.4}Mn_{1.6}O_4$ Nanoparticles

Using 10 mg/ml of 3-[4,5-dimethylthiazole-2-yl]-2,5-diphenyltetrazolium bromide as the MTT dye, $Cu_{1.4}Mn_{1.6}O_4$ nanoparticles showed. The $Cu_{1.4}Mn_{1.6}O_4$ nanoparticle samples were dissolved in 0.2% DMSO to create concentration gradients quantified in ppm at 20, 40, 80, 160, and 320. A 200 µl sample of suspended cells (1 × 10^4 cells/well) in RPMI media was distributed. The cells were cultured in 5% CO_2 for 24 hours at 37°C. The cell cultures were cultured for a further twenty-four hours under the same circumstances following treatment with 20 µl of $Cu_{1.4}Mn_{1.6}O_4$ NPs. Each sample was then incubated for five hours at 37°C with 10 µl of MTT reagent added. At 570 nm, the absorbance was measured [26].

2.4 Assay for Hemolysis Using $Cu_{1.4}Mn_{1.6}O_4$ Nanoparticles

The hemolysis assay evaluated $Cu_{1.4}Mn_{1.6}O_4$ at different concentrations (50, 250, and 500 ppm) to determine the presence of hazardous or non-toxic substances. The blood sample was obtained from the laboratory, placed in an EDTA tube, observed under a microscope at a magnification of 100, and subsequently analyzed on a slide. Following the separation of blood cells and plasma in an EDTA tube, the mixture underwent centrifugation for 10 minutes. After removing the plasma layer from the cells, the cells were subjected to a ten-minute cycle of centrifugation, during which they were continuously washed with PBS and supplemented with 1 mL of PBS. The cells were extracted from the PBS after two minutes. After multiple rounds of washing, 1 mL and 9 mL of PBS were amalgamated to create the blood cell suspension. Each tube has a volume of 1200 µL for the antagonist, administered at varying concentrations. Three hundred microliters of the cell suspension are added to the last volume (1.5 ml). Each tube is incubated for two hours before being spun apart for five minutes at 1000 cycles per minute. Then, the difference in hemolysis was quantified using control conditions (test tubes containing blood and PBS, test tubes containing blood, and deionized water only). After centrifugation, the (+) option indicates the compound's toxicity when combined with blood components. The drug was safe, as indicated by the (-) option, which shows that the blood components were not mixed after centrifugation [27].

3 RESULTS AND DISCUSSION

3.1 Characterization of $Cu_{1.4}Mn_{1.6}O_4$

Nanoparticles by FTIR: Functional groups are examined by FTIR characterization. The FTIR spectrum was utilized to analyze the chemical bonding of $Cu_{1.4}Mn_{1.6}O_4$ nanoparticles, with a wavenumber range of 400 to 4000 cm-1. Absorption peaks are seen in Figure 1, including one at a wavenumber of 442.92 cm-1, corresponding to the metal's vibrational mode within a tetrahedral structure (Cu-O) [28]. The octahedral vibration mode (Mn-O) was seen with a wave number of 524.6 cm-1 [29].

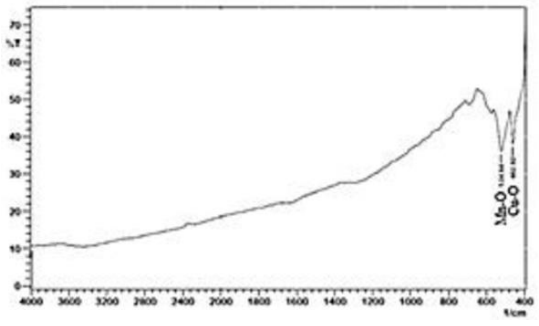

Figure 1: $Cu_{1.4}Mn_{1.6}O_4$ nanoparticles FTIR spectra.

3.2 Characterization of $Cu_{1.4}Mn_{1.6}O_4$ Nanoparticles by Dynamic Light Scattering (DLS)

The granular size of $Cu_{1.4}Mn_{1.6}O_4$ was assessed to evaluate the stability of the nanoparticles in colloidal solutions and their response to the solvent. Ionic water served as a solvent, and the particle size of $Cu_{1.4}Mn_{1.6}O_4$ was measured at 196.3 nm, as illustrated in Figure 2.

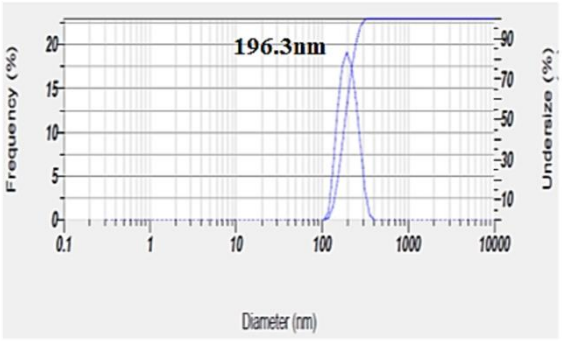

Figure 2: $Cu_{1.4}Mn_{1.6}O_4$ nanoparticles by dynamic light scattering (DLS).

3.3 Characterization of $Cu_{1.4}Mn_{1.6}O_4$ Nanoparticles by (XRD) and (EDX)

XRD was utilized to measure $Cu_{1.4}Mn_{1.6}O_4$ nanoparticles. The XRD measurements are presented in Figure 3. Among the several identified peaks at 2θ, ten are principal, with seven exhibiting sharpness and intensity, signifying a high level of $Cu_{1.4}Mn_{1.6}O_4$ crystallinity. The values of the peaks are 35.45, 37.74, 39.75, 48.34, 62.62, 65.62, 67.65, 69.82, and 77.97. The relative intensity data of the peaks on the XRD diagram aligns favourably with the parameters of $Cu_{1.4}Mn_{1.6}O_4$, as per ICCD card

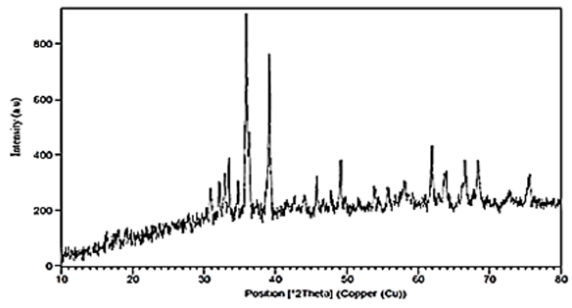

Figure 3: X-ray diffraction spectrum of $Cu_{1.4}Mn_{1.6}O_4$ nanoparticles.

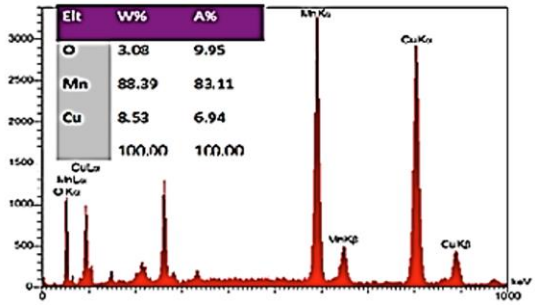

Figure 4: Energy dispersive X-rays (EDX) of $Cu_{1.4}Mn_{1.6}O_4$ nanoparticles.

standard No. (96-153-3678) and the cubic data of the Crystal system [30]. The average crystalline size was calculated to be 38.12 nm using the Debye-Scherrer equation. Energy-dispersive X-ray spectroscopy (EDX) was used to quantify $Cu_{1.4}Mn_{1.6}O_4$ synthesized utilizing green chemistry Figure 4. The results indicated the presence of copper at 36.9%, oxygen at 26.6%, and manganese at 36.5%, signifying a high purity level.

3.4 Characterization of $Cu_{1.4}Mn_{1.6}O_4$

Nanoparticles by SEM The morphological and structural compositions of $Cu_{1.4}Mn_{1.6}O_4$ nanoparticles synthesized through green chemistry were analyzed utilizing a scanning electron microscope (SEM). Figure 5 shows that the particles were prepared in the nanometer range. The SEM images demonstrated that most of the nanoparticles were adequately separated, although a portion was observed in an agglomerated state. The observed agglomeration results from electrostatic effects, with the particle diameter measuring approximately 103.60 nm [33].

3.5 Inhibition of $Cu_{1.4}Mn_{1.6}O_4$ Nanoparticles for PC3

The impact of green chemistry-prepared $Cu_{1.4}Mn_{1.6}O_4$ nanoparticles on the vitality of PC3 cell lines was investigated, and the drug Flutamide was compared. Following a 24-hour incubation period, the concentrations of the nanoparticles at 20, 40, 80, 160, and 320 ppm (the percentage of killing cancer cells, respectively) were 37.68%, 47.75%, and 63.38%. Figure 6 illustrates how $Cu_{1.4}Mn_{1.6}O_4$'s killing efficacy on cancer cells increases with concentration, reaching 87.07% and 98.00%. The results in 24 hours showed an IC50 value = 38.46, as in Figure 7.

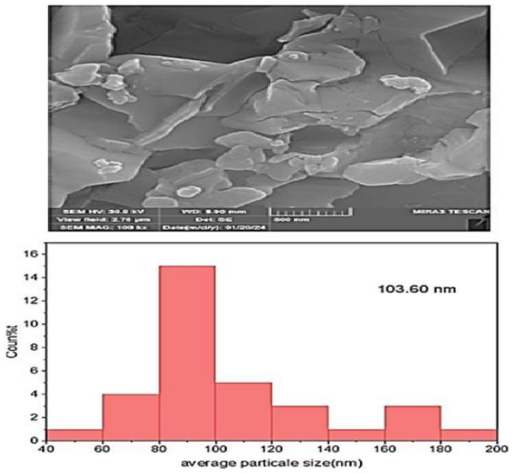

Figure 5: SEM of $Cu_{1.4}Mn_{1.6}O_4$ nanoparticles.

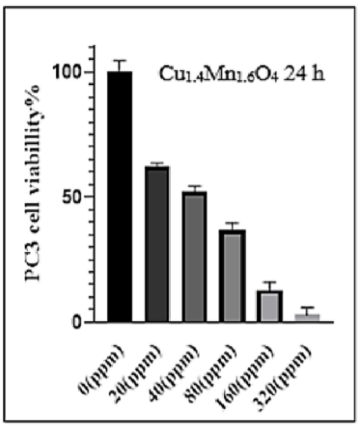

Figure 6: Inhibition of $Cu_{1.4}Mn_{1.6}O_4$ nanoparticles for PC3 in 24 h.

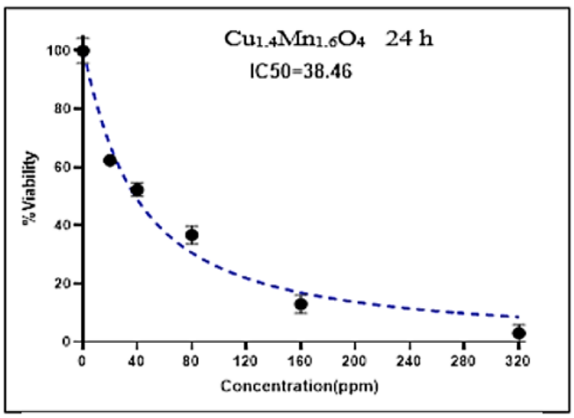

Figure 7: IC50 of $Cu_{1.4}Mn_{1.6}O_4$ nanoparticles for PC3 in 24 h.

The results of Flutamide after a 24-hour incubation at concentrations of 20, 40, 80, 160, and 320 ppm were as follows: the percentage of cancer cell mortality was 6.51%, 10.45%, 27.96%, 32.48%, and 52.53%, respectively. The lethality of $Cu_{1.4}Mn_{1.6}O_4$ nanoparticles surpasses that of Flutamide under the same doses and circumstances, as illustrated in Figure 8.

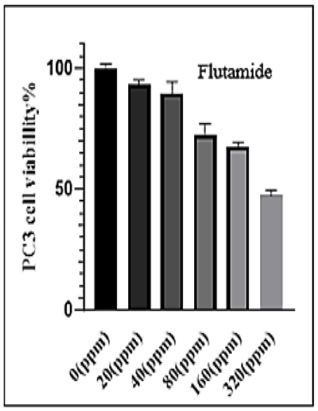

Figure 8: Inhibition of Flutamide for PC3 in 24 h.

The results showed an IC50 value of 296.8, as shown in Figure 9.

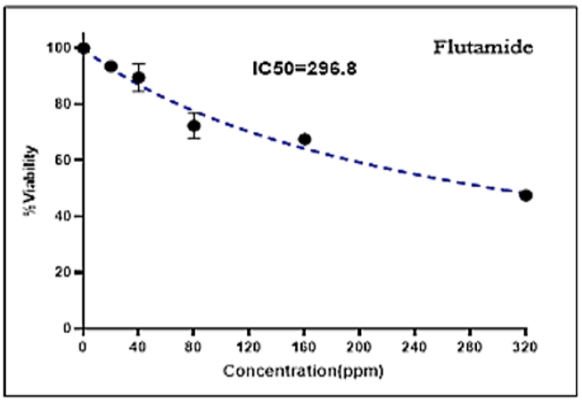

Figure 9: IC50 of Flutamide for PC3 in 24 h.

3.6. Toxicity Test of $Cu_{1.4}Mn_{1.6}O_4$ Nanoparticles on Blood Cells

Blood cells were used to investigate the cytotoxicity of $Cu_{1.4}Mn_{1.6}O_4$ Nanoparticles at 500, 250, and 50 ppm. The outcomes were compared to those of the medication Flutamide. As seen in Figure 10, the results indicated that $Cu_{1.4}Mn_{1.6}O_4$ Nanoparticles were not hazardous. However, as Figure 11 illustrates, the drug's toxicity was noted at the same concentrations as the control group.

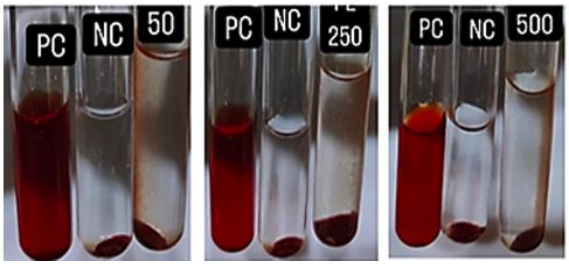

Figure 10: Hemolysis test for $Cu_{1.4}Mn_{1.6}O_4$ nanoparticle.

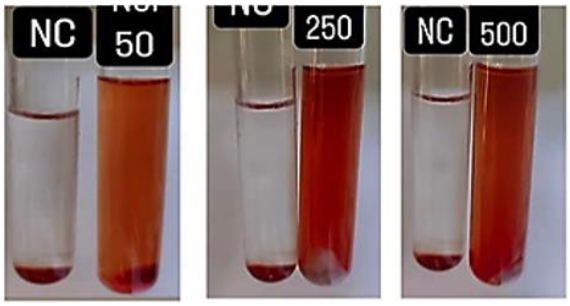

Figure 11: Hemolysis test for Flutamide nanoparticle.

Numerous studies have indicated that cellular absorption efficiency, concentrations, exposure length, and nanoparticle size may all influence the extent of NP-mediated cell death [34]. Recent data demonstrate that nanoparticles can eliminate tumour cells with minimal to no effect on the mortality of normal cells [35], [36]. Assessment of Apoptotic Evaluations Mitochondria serve as critical signalling nodes in the apoptotic pathway; thus, various apoptosis regulators may inhibit or inflict damage on mitochondria during apoptosis. Anti-apoptotic proteins, including Bcl-2 and Bcl-2 family proteins Bak and Bax, are particularly important for mitochondrial-mediated death. Additionally, extensive research has investigated the capacity of nanoparticles (NPs) to induce oxidative stress and subsequently generate reactive oxygen species (ROS) that can eliminate tumour cells [37], [38].

4 CONCLUSIONS

This work offers a fresh, reasonably priced approach for the synthesis of $Cu_{1.4}Mn_{1.6}O_4$ nanoparticles from Ginkgo biloba leaf extract. The method combines co-precipitation, green chemistry, and ultrasonic methods into one process for manufacturing nanoparticles. Using XRD, FT-IR, EDX, SEM, and DLS, among other methods, the produced nanoparticles were characterized. Although the average particle size shown in the SEM was 103.60 nm, the average size detected in the XRD was 38.12 nm. Measuring by DLS, the average particle size was 196.3 nm. On the PC3 cell line, the efficacy of the synthetic $Cu_{1.4}Mn_{1.6}O_4$ nanoparticles was assessed against the pharmacological Flutamide, used in Iraq for the therapy of prostate cancer. The findings showed the remarkable efficiency and quality of the created nanoparticles as compared to the given medicine. $Cu_{1.4}Mn_{1.6}O_4$NPs showed positive cytotoxicity against cancerous cells in the prostate. Apoptotic pathways can be triggered by treated cells. Moreover, the tumor suppressor gene p53's mRNA expression was increased by $Cu_{1.4}Mn_{1.6}O_4$NPs. The recently generated $Cu_{1.4}Mn_{1.6}O_4$NPs could be a major springboard for additional cancer treatment research. In contrast to chemotherapy, the present study's findings offer promise for stopping the spread of prostate cancer.

ACKNOWLEDGMENTS

The authors are grateful to the department for their valuable support during this study.

REFERENCES

[1] J.-Y. Zhang, L.-J. Zhao, and Y.-T. Wang, “Synthesis and clinical application of small-molecule drugs approved to treat prostatic cancer,” Eur. J. Med. Chem., vol. 262, p. 115925, 2023.

[2] G. Joshi et al., “Growth factors mediated cell signalling in prostate cancer progression: Implications in discovery of anti-prostate cancer agents,” Chem. Biol. Interact., vol. 240, pp. 120–133, 2015.

[3] F. A. Fisusi and E. O. Akala, “Drug combinations in breast cancer therapy,” Pharm. Nanotechnol., vol. 7, no. 1, pp. 3–23, 2019.

[4] C. Taylor and A. Kirby, “Cardiac side-effects from breast cancer radiotherapy,” Clin. Oncol., vol. 27, no. 11, pp. 621–629, 2015.

[5] Z. Zhang et al., “The potential of marine-derived piperazine alkaloids: Sources, structures and bioactivities,” Eur. J. Med. Chem., vol. 265, p. 116081, 2024.

[6] T. Youshikawa, Y. Naito, and M. Kondo, “Ginkgo Biloba leaf extract–review of biological actions,” Antioxid. Redox Signal., vol. 4, pp. 469–480, 1999.

[7] T. K. Mohanta, Y. Tamboli, and P. Zubaidha, “Phytochemical and medicinal importance of Ginkgo biloba L.,” Nat. Prod. Res., vol. 28, no. 10, pp. 746–752, 2014.

[8] W. Zuo et al., “Advances in the studies of Ginkgo biloba leaves extract on aging-related diseases,” Aging Dis., vol. 8, no. 6, pp. 812–823, 2017.

[9] E. Koch, "Inhibition of platelet activating factor (PAF)-induced aggregation of human thrombocytes by ginkgolides: considerations on possible bleeding complications after oral intake of Ginkgo biloba extracts," Phytomedicine, vol. 12, no. 1–2, pp. 10–16, 2005.

[10] B. Avula et al., "Identification of Ginkgo biloba supplements adulteration using HPTLC and UHPLC-DAD-QTOF-MS," Anal. Bioanal. Chem., vol. 407, pp. 7733–7746, 2015.

[11] H. S. Ahmed, M. Hammadi, and W. Majeed, "Green Synthesis of $CuCr_2O_4$Nano Composite from Rosemary Extract and Evaluation of its Anti-Breast Cancer Properties," J. Nanostruct., vol. 14, no. 4, pp. 1183–1190, 2024.

[12] M. Salah, M. Hammadi, and E. H. Hummadi, "Anticancer activity and cytotoxicity of ZnS nanoparticles on MCF-7 human breast cancer cells," Biochem. Cell. Arch., vol. 21, no. 1, 2021.

[13] W. M. Salih et al., "Green synthesis of (CeO_2)-(CuO) nanocomposite, analytical study, and investigation of their anticancer activity against Saos-2 osteosarcoma cell lines," Inorg. Chem. Commun., vol. 159, p. 111730, 2024.

[14] K. Xiao et al., "LHRH-targeted redox-responsive crosslinked micelles impart selective drug delivery and effective chemotherapy in triple-negative breast cancer," Adv. Healthc. Mater., vol. 10, no. 3, p. 2001196, 2021.

[15] D. Medina-Cruz et al., "Bimetallic nanoparticles for biomedical applications: A review," in Racing for the Surface: Antimicrobial and Interface Tissue Engineering, 2020, pp. 397–434.

[16] H. Li et al., "Modifying electrical and magnetic properties of SWCNTs by decorating with iron oxide nanoparticles," J. Nanosci. Nanotechnol., vol. 20, no. 4, pp. 2611–2616, 2020.

[17] Z. He, Z. Zhang, and S. Bi, "Nanoparticles for organic electronics applications," Mater. Res. Express, vol. 7, no. 1, p. 012004, 2020.

[18] N. O. Alafaleq et al., "Biogenic synthesis of Cu-Mn bimetallic nanoparticles using pumpkin seeds extract and their characterization and anticancer efficacy," Nanomaterials, vol. 13, no. 7, p. 1201, 2023.

[19] K. A. Elsayed et al., "Fabrication of ZnO-Ag bimetallic nanoparticles by laser ablation for anticancer activity," Alex. Eng. J., vol. 61, no. 2, pp. 1449–1457, 2022.

[20] Y. Cao et al., "Green synthesis of bimetallic ZnO–CuO nanoparticles and their cytotoxicity properties," Sci. Rep., vol. 11, no. 1, p. 23479, 2021.

[21] A. Eskandari and K. Suntharalingam, "A ROS-generating, CSC-potent Mn(II) complex and its encapsulation into polymeric nanoparticles," Chem. Sci., vol. 10, no. 33, pp. 7792–7800, 2019.

[22] H. S. Ahmed, D. N. J. Hussien, and D. F. M. Yusoff, "Synthesis, characterization, and antibacterial activity of some new metal complexes containing semicarbazide," Int. J. Appl. Sci., vol. 1, no. 1, pp. 36–49, 2024.

[23] T. Mehdizadeh, A. Zamani, and S. M. A. Froushani, "Preparation of Cu nanoparticles fixed on cellulosic walnut shell and its antibacterial, antioxidant, and anticancer effects," Heliyon, vol. 6, no. 3, 2020.

[24] K. Skłodowski et al., "Metallic nanosystems in antimicrobial strategies with high activity and biocompatibility," Int. J. Mol. Sci., vol. 24, no. 3, p. 2104, 2023.

[25] H. Y. Jassim and M. Hammadi, "Synthesis, green chemistry method characterization of $CuFe_5O_8$ nanocomposite and assessment of its prostate cancer-preventive effects," 2024.

[26] M. Hammadi, E. H. Hummadi, and R. Sabah, "Synthesis of CuS nanoparticle and investigation of their anticancer activity against a human breast cancer cell line," J. Pharm. Negat. Results, vol. 13, no. 2, 2022.

[27] P. Wayne, Clinical and Laboratory Standards Institute. Performance Standards for Antimicrobial Susceptibility Testing, 2011.

[28] A. Carrapiço et al., "Biosynthesis of metal and metal oxide nanoparticles using microbial cultures: mechanisms, antimicrobial activity and applications to cultural heritage," Microorganisms, vol. 11, no. 2, p. 378, 2023.

[29] M. R. Shaik et al., "Mn_3O_4 nanoparticles: Synthesis, characterization and their antimicrobial and anticancer activity," Saudi J. Biol. Sci., vol. 28, no. 2, pp. 1196–1202, 2021.

[30] M. Beley, L. Padel, and J. C. B., "Etudes et propriétés des composés $Cu_xMn_{3-x}O_4$ (avec x = 1, 0; 1, 2 et 1, 4)," 1978.

[31] A. A. K. Rikabi et al., "Optimization of ecofriendly L-Fe/Ni nanoparticles prepared using black tea extract for removal of tetracycline from groundwater," South Afr. J. Chem. Eng., vol. 50, pp. 89–99, 2024.

[32] M. Nasrollahzadeh, M. Sajjadi, and S. M. Sajadi, "Biosynthesis of Cu nanoparticles supported on MnO_2 using Centella asiatica extract for catalytic reduction," Chin. J. Catal., vol. 39, no. 1, pp. 109–117, 2018.

[33] R. A. Salman, M. W. M. Alzubaidy, and A. T. Tawfeeq, "Effect of Mirabilis jalapa fortified with nano-quercetin to accelerate wound healing in vivo," J. Glob. Innov. Agric. Sci., vol. 12, pp. 717–723, 2024.

[34] R. Foldbjerg et al., "PVP-coated silver nanoparticles and silver ions induce ROS, apoptosis and necrosis in THP-1 monocytes," Toxicol. Lett., vol. 190, no. 2, pp. 156–162, 2009.

[35] N. Asare et al., "Cytotoxic and genotoxic effects of silver nanoparticles in testicular cells," Toxicology, vol. 291, no. 1–3, pp. 65–72, 2012.

[36] R. H. Whitaker and W. J. Placzek, "Regulating the BCL2 family to improve sensitivity to microtubule targeting agents," Cells, vol. 8, no. 4, p. 346, 2019.

[37] R. Pati et al., "Zinc-oxide nanoparticles exhibit genotoxic, clastogenic, and cytotoxic effects via oxidative stress," Toxicol. Sci., vol. 150, no. 2, pp. 454–472, 2016.

[38] B. Hamed et al., "A comprehensive investigation using laser ablation method for analyzing nanocomposite anticancer properties," BioNanoScience, vol. 15, no. 1, p. 96, 2025.